

1 **Title:** Inactivation of *Burkholderia cepacia* complex phage KS9 gp41 identifies the phage  
2 repressor and generates lytic virions.

3

4 **Running Title:** *Burkholderia cepacia* phage KS9

5

6 **Authors:**

7 Karlene H. Lynch<sup>1</sup>

8 Kimberley D. Seed<sup>1</sup>

9 Paul Stothard<sup>2</sup>

10 Jonathan J. Dennis\*<sup>1</sup>

11

12 **Affiliations:**

13 <sup>1</sup>Department of Biological Sciences, University of Alberta, Edmonton, Alberta, Canada

14 <sup>2</sup>Department of Agricultural, Food and Nutritional Science, University of Alberta, Edmonton,

15 Alberta, Canada

16

17 **\*Corresponding author:**

18 Department of Biological Sciences, University of Alberta, Edmonton, Alberta, Canada T6G 2E9

19 Telephone: (780) 492-2529; Fax: (780) 492-9234; E-mail: jon.dennis@ualberta.ca

20

21

22

23

24 **Abstract**

25           The *Burkholderia cepacia* complex (Bcc) is made up of at least seventeen species of  
26 Gram-negative opportunistic bacterial pathogens that cause fatal infections in patients with cystic  
27 fibrosis and chronic granulomatous disease. KS9 (vB\_BcenS\_KS9), one of a number of  
28 temperate phages isolated from Bcc species, is a prophage of *Burkholderia pyrrocinia* LMG  
29 21824. Transmission electron micrographs indicate that KS9 belongs to the family *Siphoviridae*  
30 and exhibits the B1 morphotype. The 39,896 base pair KS9 genome, comprised of 50 predicted  
31 genes, integrates into the 3' end of the LMG 21824 GTP cyclohydrolase II open reading frame.  
32 The KS9 genome is most similar to uncharacterized prophage elements in the genome of *B.*  
33 *cenoepecia* PC184 (vB\_BcenZ\_PC184), as well as *Burkholderia thailandensis* phage  $\phi$ E125  
34 and *Burkholderia pseudomallei* phage  $\phi$ 1026b. Using molecular techniques we have disrupted  
35 KS9 gene *41*, which exhibits similarity to genes encoding phage repressors, producing a lytic  
36 mutant named KS9c. This phage is incapable of stable lysogeny in either LMG 21824 or *B.*  
37 *cenoepecia* strain K56-2, and rescues a *Galleria mellonella* infection model from experimental  
38 *B. cenoepecia* K56-2 infections at relatively low multiplicities of infection. These results  
39 readily demonstrate that temperate phages can be genetically engineered to lytic form and that  
40 these modified phages can be used to treat bacterial infections *in vivo*.

41  
42  
43  
44

## 45 Introduction

46 The *Burkholderia cepacia* complex (Bcc) is a group of at least seventeen Gram-negative  
47 species, the first identified strains of which were characterized as onion pathogens by W. H.  
48 Burkholder (9). While these bacteria have a number of beneficial activities, including the  
49 promotion of crop growth and the degradation of organic pollutants, they have gained notoriety  
50 in the last two decades as serious opportunistic pathogens (19, 21, 25). Bcc species, particularly  
51 *B. multivorans* and *B. cenocepacia*, cause serious respiratory infections in patients with cystic  
52 fibrosis and chronic granulomatous disease (42, 7). These infections are especially problematic  
53 due to symptom severity, the inherent antibiotic resistance of Bcc species, and the potential for  
54 rapid spread through susceptible patient populations (25, 23). Difficulties in treating these  
55 infections have led to the unfortunate practice of segregating patients, which has high economic,  
56 social, and psychological costs (18).

57 Because of these clinical difficulties, interest in the isolation and characterization of  
58 *Burkholderia*-specific bacteriophages (or phages) has increased in recent years, with the apparent  
59 potential for using phages as therapeutic agents. Phage therapy is the clinical application of  
60 phages to prevent and/or to treat infections, which offers a promising alternative to antibiotic  
61 treatment for resistant bacteria such as those of the Bcc (33, 39). A second benefit of these phage  
62 studies is that they may provide insight into the possible mechanisms of Bcc virulence. For  
63 example, BcepMu, a transposable phage that specifically infects strains of *B. cenocepacia*, was  
64 found to carry genes similar to *exeA*, involved in toxin secretion, and *mdmB* and *oafA*, two  
65 acyltransferases (44). Finally, as *Burkholderia* phages tend to be underrepresented in  
66 comparative studies with respect to *Escherichia coli* and lactic acid bacteria phages, Bcc-specific  
67 phage studies provide novel information about a relatively uncharacterized group of viruses.

68           Although phage therapy using temperate virions can be effective (39), there are several  
69 reasons why lytic phages are generally considered the most appropriate candidates for use in  
70 phage therapy. One of the concerns is that phage integration can lead to lysogenic conversion  
71 and enhanced virulence (8). A second concern is that integration of temperate phages results in  
72 superinfection immunity due to expression of the phage repressor from the prophage. This  
73 protein binds to the operators of infecting phage DNA and represses gene expression, preventing  
74 both the initiation of the lytic cycle and the establishment of lysogeny (14). A third concern is  
75 that lysogeny affects the kinetics of infection. When a phage infects a cell and undergoes  
76 lysogeny instead of entering the lytic cycle, the cell survives and no new phage particles are  
77 released (27). A final problem is that prophages can lead to specialized transduction following  
78 induction. Specialized transduction occurs following inexact excision of a prophage from the  
79 bacterial chromosome. Bacterial DNA flanking the prophage is packaged into the capsid, and  
80 this sequence, which can potentially encode virulence factors, can subsequently recombine into  
81 the chromosome of a new host (14).

82           It has been estimated that more than half of tailed phages have evolved a temperate  
83 lifestyle, although some estimates have been greater than 90% (1, 22). This situation makes the  
84 isolation of naturally lytic phages extremely difficult, particularly when they must have a specific  
85 host range that includes clinically relevant bacterial species, such as *B. cenocepacia* (24). The  
86 use of classical genetics to produce lytic phage variants, for example by plating temperate phages  
87 on lysogens and screening for clear plaque *vir* mutants, is complicated by the fact that such  
88 mutations are undefined.

89           This report describes the characterization of KS9 (vB\_BcenS\_KS9), a prophage of  
90 *Burkholderia pyrrocinia* LMG 21824 (41), and its conversion to a lytic phage through specific

91 molecular modification of gene *41* encoding its putative lytic phase repressor. Preliminary  
92 characterization of short sequences by Seed and Dennis (41) indicated that the genome of KS9,  
93 whose host range includes Bcc *B. cenocepacia* K56-2, shows similarity to the genomes of two  
94 non-Bcc *Burkholderia* phages:  $\phi$ E125, a prophage of *Burkholderia thailandensis* E125 (47), and  
95  $\phi$ 1026b, a prophage of *Burkholderia pseudomallei* 1026b (17). However, no phages closely  
96 related to KS9 have been functionally tested to demonstrate that proteins similar to gp41 function  
97 as true phage repressors. In this study, we have used the Bcc infection model of *Galleria*  
98 *mellonella* (40) to assess both the contribution of the KS9 prophage to Bcc host virulence and the  
99 ability of a genetically modified KS9 to treat *B. cenocepacia* infections without stably integrating  
100 into the host bacterial chromosome as a prophage.

101

## 102 **Materials and Methods**

### 103 Bacterial strains and growth conditions

104 *Burkholderia cenocepacia* K56-2 and *Burkholderia pyrrocinia* LMG 21824 are members  
105 of the Bcc experimental strain panel (32) and the updated Bcc strain panel (13), obtained from  
106 Belgium Coordinated Collection of Microorganisms LMG Bacteria Collection (Ghent, Belgium)  
107 and the Canadian *Burkholderia cepacia* Complex Research and Referral Repository (Vancouver,  
108 BC, Canada). K56-2 LPS mutants were a kind gift from Miguel Valvano (University of Western  
109 Ontario, London, ON, Canada). These strains were grown aerobically overnight at 30°C on half-  
110 strength Luria-Bertani (½ LB) solid medium or broth. Transformations were performed with  
111 chemically-competent DH5 $\alpha$  (Invitrogen, Carlsbad, CA). Transformed DH5 $\alpha$  were plated on LB  
112 medium containing 100  $\mu$ g/ml ampicillin or 100  $\mu$ g/ml trimethoprim and 15  $\mu$ g/ml tetracycline  
113 and grown overnight at 37°C. Electroporations were performed using a Bio-Rad MicroPulser

114 (Bio-Rad, Hercules, CA) and were plated on half-strength LB medium containing 300 µg/ml  
115 trimethoprim and 300 µg/ml tetracycline. Strains were stored at -80°C in LB medium containing  
116 20% glycerol.

117

#### 118 Electron microscopy

119       Overnight cultures of LMG 21824 were pelleted by centrifugation at 10,000 x g for 2  
120 min. The supernatant was filter sterilized using a 0.45 µm filter. This solution was incubated on a  
121 carbon grid for 5 min. at room temperature and then stained with 2% phosphotungstate. A  
122 Philips/FEI (Morgagni) Transmission Electron Microscope with CCD camera was used to take  
123 the KS9 micrograph, with the assistance of the University of Alberta Department of Biological  
124 Sciences Microscopy Service Unit.

125

#### 126 KS9 propagation and DNA isolation

127       KS9 was isolated by Seed and Dennis (41) from a single plaque on a lawn of *B.*  
128 *pyrocinia* LMG 21824. Phage stocks were prepared in 1.5 ml of suspension media (50 mM  
129 Tris/HCl, pH 7.5, 100 mM NaCl, 10 mM MgSO<sub>4</sub>, 0.01% gelatin solution) containing KS9  
130 plaques isolated using a sterile Pasteur pipette. Following addition of CHCl<sub>3</sub> and incubation for 1  
131 hour at room temperature, stocks were stored at 4°C. Propagation and plaque assays of KS9 were  
132 performed as described previously (41). One hundred microliters of phage stock was incubated  
133 for 20 min. at room temperature with 100 µl of *B. cenocepacia* K56-2 overnight culture.  
134 Following the addition of 3 ml of soft nutrient agar, this mixture was poured onto half-strength  
135 LB medium and grown overnight at 30°C. For EOP determinations, this procedure was repeated  
136 in three separate trials. For DNA isolation, plates of half-strength LB medium showing confluent

137 KS9 lysis were prepared as described above using 100  $\mu$ l of a KS9 high titer stock, 100  $\mu$ l of  
138 K56-2, and 3 ml of soft nutrient agarose. Phages were isolated from these plates by overlaying  
139 with suspension media and the DNA was extracted using the Wizard Lambda Preps DNA  
140 Purification System (Promega, Madison, WI).

141

#### 142 Library construction and sequence analysis

143 KS9 DNA was digested with EcoRI and Sall (Invitrogen) and the restriction fragments  
144 were separated on 0.8% (w/v) agarose gels in 1X Tris-Acetate-EDTA (pH 8.0). These fragments  
145 were purified using the GENECLEAN II Kit (Qbiogene, Irvine, CA) and ligated into pUC19.  
146 Blue/white selection was performed on LB medium containing 100  $\mu$ g/ml ampicillin after  
147 transformation of the constructs into DH5 $\alpha$ . Constructs were isolated using a QIAprep Miniprep  
148 Kit (QIAGEN, Hilden, Germany). The presence of an insert in pUC19 was verified by restriction  
149 digest and agarose gel electrophoresis. The sequencing of plasmid inserts was performed on an  
150 ABI 3100 Genetic Analyzer (Applied Biosystems, Foster City, CA) by the University of Alberta  
151 Department of Biological Sciences Molecular Biology Service Unit.

152 Sequences were edited with EditView (PerkinElmer, Waltham, MA) and aligned into a  
153 single contig using AutoAssembler (PerkinElmer). A total of 327 sequences were used, with an  
154 assembled length of 39,896 base pairs (bp). Primers (Sigma-Genosys, Oakville, ON, Canada)  
155 designed to amplify internal regions of the plasmid inserts were used for primer walking. Gaps  
156 between sequences were filled by PCR amplification and cloning and sequencing of the resulting  
157 amplicons using the TOPO TA Kit (Invitrogen). This protocol was also used to sequence the  
158 KS9 insertion sites (LMG 21824 forward primer, 21824F: CCCACGCGCTACGGTACG; KS9  
159 reverse primer, KS9R: CCGATGTAGTCCAGGCACACC; KS9 forward primer, KS9F:

160 CACTGGGCGCCCGTTGAG; LMG 21824 reverse primer, 21824R:  
161 AGGTTGGTGTCTCGCCGTCC). PCR was performed with an Eppendorf Mastercycler gradient  
162 DNA thermal cycler (Eppendorf, Hamburg, Germany) using TopTaq DNA polymerase  
163 (QIAGEN) and the recommended reaction composition and cycling conditions.

164 To identify the putative overlap region of the KS9 *attP* site, the sequence between gene  
165 *30* and the integrase gene, *31*, was analyzed using BLASTN. This region showed 71% identity  
166 with a 207 bp region (1155342-1155547) of *Burkholderia lata* 383 chromosome 2 (also known  
167 as ATCC 17760/LMG 22485). This region of similarity is longer than *attL* because it includes  
168 both *attL* and a downstream region similar to KS9. The *Burkholderia lata* 383 DNA sequence  
169 flanking the similar region was used to design primers for amplification of the junction between  
170 the LMG 21824 genome sequence and the 5' end of the KS9 prophage. The site of integration  
171 was then verified by sequencing this amplicon and a second amplicon from the 3' KS9/LMG  
172 21824 junction. The K56-2/5' KS9 junction in K56-2::KS9 was also identified using this  
173 procedure.

174 The assembled sequences were analyzed using the NCBI suite of programs. Annotation  
175 was performed using this suite, including BLASTX (3, <http://blast.ncbi.nlm.nih.gov/>) and ORF  
176 Finder (<http://www.ncbi.nlm.nih.gov/gorf/gorf.html>), and GeneMark.hmm-P (30,  
177 <http://exon.biology.gatech.edu/>) (Table 1). In all cases (except genes *12* [expressed by a  
178 translational frameshift] and *24'* [a gene embedded in *24*]), the manual assignments matched the  
179 GeneMark results. Gene and gene product numbers were assigned based on the numbering  
180 system of  $\phi$ E125/ $\phi$ 1026b. The predicted KS9 protein most similar to gp2 of these phages was  
181 assigned the name gp2 and the gene encoding this product was named gene 2. Subsequent  
182 proteins were named gp3, etc. Protein transmembrane domains were identified using OCTOPUS

183 (46, <http://octopus.cbr.su.se/>). Stem-loop structures were identified using mfold (50,  
184 <http://mfold.bioinfo.rpi.edu/>). Signal peptide cleavage sites were identified using LipoP (26,  
185 <http://www.cbs.dtu.dk/services/LipoP/>). The sequences of KS9,  $\phi$ 1026b and *B. cenocepacia*  
186 PC184 were compared using the Artemis Comparison Tool (11). The KS9 genome map was  
187 prepared using GenVision (DNASTAR, Madison, WI).

188

#### 189 Mutagenesis and *Galleria mellonella* infection

190 Plasmid pKL1 was created by ligating pALTER-1 (Promega) to an EcoRI/KpnI PCR  
191 amplicon of KS9 base pairs 5054-6078 (EcoRI<sub>F</sub>: AAGAATTCAGCGCGGCATCG; KpnI<sub>R</sub>:  
192 TTGGTACCCGCCGTGTGCTTG), the 630 bp KpnI fragment of p34S-Tp2 (15, 16), and a  
193 KpnI/BamHI PCR amplicon of KS9 base pairs 6481-7580 (KpnI<sub>F</sub>:  
194 AAGGTACCGTCTGCAATTCAATAGC; BamH<sub>I</sub><sub>R</sub>: TTGGATCCTTGGTGCTTTCTCG).  
195 LMG 21824 was electroporated with pKL1 and mutants with a single crossover (LMG  
196 21824::pKL1) were selected for on LB medium containing 300  $\mu$ g/ml trimethoprim and 300  
197  $\mu$ g/ml tetracycline. Construction of LMG 21824 (KS9 32) has been described previously (31).  
198 Briefly, an internal gene 32 segment was amplified and ligated into the *oriR*/Tp<sup>R</sup> of pTnMod-  
199 OTp' (15). This construct was electroporated into LMG 21824 and transformants were selected  
200 on LB medium containing 300  $\mu$ g/ml trimethoprim. To isolate phages from LMG 21824::pKL1,  
201 overnight cultures of these mutants were pelleted by centrifugation at 10,000 x g for 2 min. and  
202 the supernatant was filter sterilized using a 0.45  $\mu$ m filter. Plaque assays were performed as  
203 described above and single plaques to be screened were added to 500  $\mu$ l of suspension media.  
204 PCR screening was performed using the primers 40F (TCGTGACTGGCTGTTTTTCGGAC) and  
205 42R (GCGGCCAATTTACAGAGTCG). The TopTaq DNA polymerase reaction composition

206 and cycling protocol were used with the replacement of template DNA by 1 µl of phage  
207 suspension.

208 To isolate KS9- and KS9c-insensitive K56-2 (including K56-2::KS9), plates of K56-2  
209 and KS9 or K56-2 and KS9c exhibiting confluent lysis were prepared as described above and  
210 incubated overnight at 30°C. Plates were overlaid with 3 ml of water and placed on a rocking  
211 platform at 4°C for 4 hours. The water was recovered and the cells were pelleted by  
212 centrifugation at 10,000 x g for 2 min. The supernatant was removed and the cells were  
213 resuspended in water and plated on half-strength LB medium. Single colonies were isolated and  
214 colony PCR was used to screen for lysogeny using primers 21824F and KS9R. In this procedure,  
215 prior to addition of Taq in the TopTaq protocol, a colony is added to the reaction mixture,  
216 incubated at 99.9°C for 5 min. and cooled on ice.

217 We followed the procedure for *G. mellonella* infection and treatment outlined by Seed and  
218 Dennis (39, 40). Briefly, 1 ml of an overnight culture of K56-2 or K56-2::KS9 was pelleted by  
219 centrifugation at 10,000 x g for 2 min. and resuspended in 1 ml of 10 mM MgSO<sub>4</sub> supplemented  
220 with 1.2 mg/ml ampicillin. To compare the virulence of K56-2 and K56-2::KS9, serial dilutions  
221 from 10<sup>1</sup> to 10<sup>7</sup> (bacterial concentrations of approximately 10<sup>6</sup> cells/5 µl to 10<sup>0</sup> cells/5 µl,  
222 respectively) were made in MgSO<sub>4</sub>/ampicillin solution. *G. mellonella* larvae were stored at 4°C  
223 and warmed to room temperature prior to infection. Infections were performed using a 250 µl  
224 syringe fitted with a reproducibility adapter (Hamilton, Reno, NV). For each larva, 5 µl of  
225 serially diluted bacteria was injected into the hindmost left proleg. This procedure was repeated  
226 with ten larvae for each dilution. Ten control larvae were injected with MgSO<sub>4</sub>/ampicillin  
227 solution. Larvae were incubated at 30°C and mortality was recorded 48 hours post-infection.  
228 This protocol was repeated three times for each strain. Standard deviations were calculated using

229 Microsoft Excel. To assess the activity of KS9 and KS9c in *G. mellonella*, phage lysates were  
230 first passaged through Pierce Detoxi-Gel Endotoxin Removal Gel (Thermo Scientific, Rockford,  
231 IL) and dilutions were made in MgSO<sub>4</sub>/ampicillin solution. Larvae were injected with 5 µl of a  
232 1:10<sup>4</sup> dilution of K56-2 into the hindmost left proleg and 5 µl of a 1:10<sup>0</sup>, 1:10<sup>1</sup> or 1:10<sup>2</sup> dilution  
233 of phage into the second hindmost left proleg. Ten control larvae were injected with K56-2 and  
234 MgSO<sub>4</sub>/ampicillin solution and ten control larvae were injected with undiluted phage and  
235 MgSO<sub>4</sub>/ampicillin solution. Larvae were incubated at 30°C and mortality was recorded 48 hours  
236 post-infection. This protocol was repeated three times for each MOI tested. To isolate K56-2  
237 from KS9- and KS9c-treated larvae, hemolymph was extracted from larvae surviving 48 hours  
238 post-infection using a 20 gauge needle. Serial dilutions were made in MgSO<sub>4</sub>/ampicillin solution  
239 and cells were plated on half-strength LB medium containing 100 µg/ml ampicillin.

240

## 241 **Results and Discussion**

### 242 Plaque and virion morphology

243 Seed and Dennis (41) originally isolated KS9 from a culture of *B. pyrocinia* LMG  
244 21824. Induction with ultraviolet light or mitomycin C was not necessary. When propagated on  
245 *B. cenocepacia* K56-2, KS9 forms small clear plaques, 0.3-1.0 mm in diameter. To the best of  
246 our knowledge, KS9 is unable to form plaques on *B. mallei* (10 strains tested), *B. pseudomallei*  
247 (10 strains tested) or *B. thailandensis* (4 strains tested). Transmission electron microscopy  
248 indicates that KS9 has the B1 morphotype of the family *Siphoviridae* in the order *Caudovirales*  
249 (Figure 1) (2). The virion is comprised of an icosahedral head (with a diameter of 75 nm) and a  
250 long, non-contractile tail (with a length of 250 nm). The phage particles were highly fragile, as a  
251 large number of intact capsids were visible in which the tail had broken off close to or at the

252 head/tail adaptor. The KS9 virion is larger than that of both  $\phi$ E125 (63 nm head diameter, 203  
253 nm tail length) and  $\phi$ 1026b (56 nm head diameter, 200 nm tail length) (47, 17).

254

#### 255 Receptor binding

256 To determine if LPS is involved in KS9 adhesion, K56-2 LPS mutant strains were tested  
257 in a plaque assay with high-titre stocks of KS9 and KS5 (a second Bcc phage isolated by Seed  
258 and Dennis [41]). While KS5 produced confluent lysis on strains XOA7 (*waaL*::pGP $\Omega$ Tp, EOP:  
259 0.8), XOA15 (*wabR*::pGP $\Omega$ Tp, EOP: 1.3), XOA17 (*wabS*::pGP $\Omega$ Tp, EOP: 1.1), RSF19  
260 (*wbxE*::pGP $\Omega$ Tp, EOP: 0.5) and K56-2 (EOP: 1), KS9 was unable to form plaques on any of  
261 these strains (29, 35). Both phages are likely to use the LPS as a receptor because neither phage  
262 was able to lyse the LPS mutants XOA8 (*wabO*::pGP $\Omega$ Tp) or CCB1 (*waaC*::pGP $\Omega$ Tp) (35).  
263 These results suggest that KS9 requires a relatively complete LPS structure in order to infect  
264 K56-2, likely binding to an LPS component located distal to lipid A, while KS5 likely binds to a  
265 receptor located deeper within the LPS, proximal to lipid A. These results must be interpreted  
266 cautiously because, as the mutations have caused significant deficits in LPS structure, the overall  
267 organization of the outer membrane may have been altered as well (29). Although these results  
268 are consistent with both KS9 and KS5 using LPS components as receptors, further experiments  
269 are required in order to exclude the possibility of adhesion to other outer membrane structures.

270

#### 271 Characterization of the KS9 genome

272 The KS9 genome is 39,896 base pairs (bp) in length and encodes 50 putative protein-  
273 coding genes (Table 1). The G+C content of the genome is 60.7%, which is identical to that of  
274  $\phi$ 1026b and slightly lower than that of  $\phi$ E125 (61.2%) (17, 47). The majority of the start codons

275 are ATG (42/50), with fewer GTG (8) present. Most stop codons are TGA (30/50) with equal  
276 numbers of both TAA and TAG codons (10 each). Each of the predicted KS9 proteins has some  
277 degree of similarity to other proteins, as determined by a BLASTX search, except for gp36,  
278 gp38, and gp39. The protein with the lowest detectable similarity to others is gp46, putatively  
279 involved in replication, which has 23% identity with a phage O protein of *Salmonella enterica*  
280 subsp. *enterica* serovar Javiana str. GA\_MM04042433. The predicted proteins most similar to  
281 database entries are gp13, the tail length tape measure protein, and gp18, a tail component  
282 protein. Both of these proteins have 97% identity with proteins encoded by the *B. cenocepacia*  
283 PC184 genome.

284       The KS9 genome exhibits a modular organization (Figure 2). Module boundaries were  
285 assigned based on BLASTX predictions of gene function, so KS9 genes encoding hypothetical  
286 proteins were not grouped as part of a module unless the flanking genes encoded two proteins  
287 with similar functions (as is the case for genes 6 and 15). The smallest module, which encodes  
288 proteins involved in replication, is made up of two genes, 45 and 46. The DNA packaging/head  
289 morphogenesis module is made up of genes 2-7. Although the predicted product of gene 6 has  
290 not been assigned a putative function, it is included as part of this module because of its location.  
291 Similarly, genes 10-19 comprise the tail morphogenesis module. Gene 15, encoding a  
292 hypothetical protein, has been included here because of its position. The fourth module in the  
293 genome, involved in lysis, includes genes 22-24', which encode the putative holin, endolysin, Rz  
294 and Rz1 proteins. The sequence has been deposited in GenBank, with accession number  
295 NC\_013055.1.

296

297 Similarity to *B. cenocepacia* PC184

298 The predicted gene products of KS9 are most similar to those of a prophage from *B.*  
299 *cenocepacia* PC184 (vB\_BcenZ\_PC184; Table 1, Figure 3). As shown in Table S1, the genes  
300 encoding gp1-4, gp7-19, gp22-24', gp26-28, gp45 and gp49 all have similar genes in a single  
301 locus in PC184, spanning ORFs BCPG\_00009 to BCPG\_00033. An exception is KS9 gene 15,  
302 which encodes a protein similar to PC184 BCPG\_01060. For those instances in which the PC184  
303 proteins are more closely related than predicted proteins from any other source, percent identities  
304 of the proteins range from 60% (gp45) to 97% (gp13 and gp18) (Table 1). These proteins are  
305 involved in DNA packaging/head assembly, tail assembly, lysis, replication and endonuclease  
306 activity. Casjens (12) outlines several standards by which one can predict whether a bacterial  
307 genomic sequence contains a prophage. These include a) the presence of phage-related genes  
308 (especially those required for morphogenesis), b) continuous organization undisturbed by non-  
309 phage related genes, c) characteristic prophage gene order and d) the presence of genes encoding  
310 hypothetical proteins (especially if phage-related). Using the standards put forward by Casjens  
311 (12) for identification of prophage sequences, this locus in PC184 appears to contain an  
312 uncharacterized prophage or prophage element: it contains multiple phage genes (including  
313 morphogenesis genes), the organization is continuous, the genes encoding proteins similar to  
314 those in KS9 are present in the same order as the genes in the KS9 prophage, and genes encoding  
315 proteins similar to phage-related hypothetical proteins (such as KS9 gp1) are present.

316

#### 317 Characterization of the KS9 prophage insertion site

318 Because of the similarities between KS9,  $\phi$ E125, and  $\phi$ 1026b, it was predicted that the  
319 overlap region of the KS9 *attP* would be located at a similar position in the chromosome  
320 (upstream of the integrase gene) and that it would facilitate integration into a similar locus, likely

321 the 3' end of a tRNA<sup>Pro-3</sup> coding region (47, 17). While the position of the KS9 *attP* is similar to  
322 those of both  $\phi$ E125 and  $\phi$ 1026b (upstream of the integrase gene), it facilitates recombination  
323 into a different host target gene. Using a 20 bp *attP* overlap region (Figure 4), KS9 integrates  
324 into the 3' end of a gene encoding the LMG 21824 or K56-2 GTP cyclohydrolase II (GCHII)  
325 enzyme. GCHII is responsible for the production of 2,5-diamino-6- $\beta$ -ribosyl-4(3H)-  
326 pyrimidinone 5'-phosphate from GTP. This product is the first intermediate in the synthesis of  
327 riboflavin, which is necessary for metabolism (38). The GCHII ORF lies immediately upstream  
328 of an ORF encoding a GCN5-related N-acetyltransferase (GNAT). Because phage integration  
329 does not disrupt the sequence of the predicted GCHII ORF (with the *attP* overlap region  
330 replacing the last 19 bp of the gene, including the stop codon), it suggests that there is no loss of  
331 GCHII function in a KS9 lysogen.

332 To our knowledge, there are no other published reports of prophage integration into a  
333 bacterial GCHII gene. However, we have identified a sequence in GenBank that strongly  
334 suggests that prophage insertion can occur at this site in other Bcc genomes. In chromosome 2 of  
335 *B. cenocepacia* AU 1054, ORF *Bcen\_3636* (encoding GCHII) is located 5' to ORF *Bcen\_3637*  
336 (encoding GNAT), separated by 125 bp. In contrast, the distance separating these genes in  
337 *Burkholderia lata* 383 (*Bcep18194\_B1027* GCHII [1154713-1155363] and *Bcep18194\_B1047*  
338 [1174320-1174886] GNAT) is 18,957 bp. Between these two genes in *Burkholderia lata* 383, the  
339 annotated sequence contains an additional 19 genes including a phage integrase  
340 (*Bcep18194\_B1028*), a terminase (*Bcep18194\_B1042*), a lytic transglycosylase  
341 (*Bcep18194\_B1044*), and 16 other genes without assigned functions.

342 In order to characterize this region further, we analyzed the sequence of this region  
343 beginning with the GCHII start codon and ending with the GNAT stop codon using GeneMark

344 (30). Proteins similar to the proteins encoded by GeneMark-predicted ORFs were found using  
345 BLASTX. Thirty-six ORFs were found by GeneMark, including the GCHII (ORF 1) and GNAT  
346 (ORF 36). According to BLASTX analysis, proteins encoded by 16 of the ORFs predicted by  
347 GeneMark are similar to phage-related proteins (Table S2). These include proteins from phages  
348 that infect both Gram-positive (such as *Lactococcus*) and Gram-negative (such as *Burkholderia*)  
349 bacteria. Interestingly, predicted products of four of these ORFs (3, 17, 19 and 32) are similar to  
350  $\phi$ E125 and  $\phi$ 1026b proteins, respectively: gp33/gp32 (ORF 32), gp36 of  $\phi$ 1026b (ORF 3),  
351 gp60/gp71 (ORF 17), and gp65/gp76 (ORF 19). Only one of these sets, gp33/gp32, is similar to a  
352 gene present in KS9, gp28. These data suggest that an uncharacterized prophage has integrated  
353 into *Burkholderia lata* 383 at the same (or at a similar) site as KS9 and that this phage is at least  
354 partially related to KS9. Because of its small size, it is not known if this prophage is defective or  
355 if it has retained all of the elements necessary for a productive lytic cycle. Again, using Casjens  
356 (12) parameters for prophage localization, the region we have identified in *Burkholderia lata* 383  
357 meets these requirements: a) genes encoding such phage proteins as integrase, terminase and  
358 virion morphogenesis factors are present, b) there are no obvious non-phage genes in the almost  
359 19 kbp sequence, c) the gene order is consistent with prophage organization, with the genes  
360 encoding the proteins similar to  $\phi$ 1026b gp36-gp76 to the 5' of the gene encoding the protein  
361 similar to gp32 (as in the  $\phi$ 1026b prophage) and d) genes encoding proteins similar to phage-  
362 related hypothetical proteins are present.

363

364

365 Analysis of KS9 morphogenesis genes

366 The predicted DNA packaging/head assembly proteins of KS9 are similar to those  
367 encoded by PC184,  $\phi$ E125 and  $\phi$ 1026b, but the major capsid protein itself is dissimilar (Table 1  
368 and 2). Each putative KS9 tail protein has a similar protein encoded by PC184,  $\phi$ E125 and  
369  $\phi$ 1026b. As discussed above, although KS9 gene *15* is assumed to be part of the tail  
370 morphogenesis module because of its location, its predicted product does not have an assigned  
371 function and so may not be involved in tail production. In many phage genomes, two proteins are  
372 encoded between the major tail protein and tail tape measure genes by way of a -1 translational  
373 frameshift (48). It is thought that frameshifting allows phages to control the relative expression  
374 levels of two proteins during infection (48). In KS9, these two proteins are gp11, a tail assembly  
375 chaperone, and gp12, a minor tail protein. These proteins are predicted to have the same N-  
376 terminal sequence, but gp12 (expressed via the frameshift) is predicted to be longer and have a  
377 different C-terminus. We have found a putative frameshift site between bases 20,347 and 20,353.  
378 This site contains a stretch of seven adenine residues that can cause the ribosome to slip  
379 backwards by one position, resulting in a -1 frameshift. Although AAAAAAA is not the  
380 canonical frameshift sequence (XXXYYYYZ, where Y is A or T), it is the same sequence that was  
381 identified for phages such as c2 of *Lactococcus* and PSA of *Listeria monocytogenes* (48).  
382 Providing further support that this is the correct frameshift sequence, we have used the mfold  
383 program to identify a potential stem-loop structure formed by 65 downstream bases (50; Figure  
384 5). Although such structures are not necessarily found at frameshift sites, their presence suggests  
385 a mechanism by which the ribosome may stall and subsequently change its reading frame (48).  
386  
387  
388 Analysis of KS9 lysis genes

389 KS9 encodes four proteins putatively involved in lysis, all of which are similar to  
390 proteins from PC184, but not  $\phi$ E125 or  $\phi$ 1026b (Table S1). The genes encoding these proteins  
391 are part of a single module (Figure 2). The first gene in the module, gene 22, encodes a putative  
392 holin. Class I holins, such as  $\lambda$  S, have three transmembrane domains, while class II holins only  
393 have two (49). Because OCTOPUS analysis (46) indicates that gp22 has three transmembrane  
394 domains, we predict that this protein is a class I holin. Phage lysins may be one of three major  
395 types: endo- $\beta$ -N-acetylglucosaminidases or N-acetylmuramidases, endopeptidases, or N-  
396 acetylmuramyl-L-alanine amidases (20). We predict that the KS9 lysin is an endopeptidase: the  
397 putative lysin, gp23, is similar to M15A peptidases and is predicted to belong to the  
398 Peptidase\_M15\_3 superfamily (E-value =  $2e^{-23}$ ). The KS9 Rz/Rz1 pair is the last gene segment  
399 in the lysis module. Rz/Rz1 proteins function in lysis by joining the inner and outer membranes  
400 following holin insertion and lysin activity (5). The Rz1 gene, 24', is located out of frame in the  
401 Rz gene, 24. Using the LipoP program (26), it is predicted that a signal-peptidase II cleavage site  
402 is present between residues 22 (alanine) and 23 (cysteine) of gp24'. Cleavage at this site would  
403 produce a 65 amino acid lipoprotein. Of these 65 amino acids, 7 are proline (10.8%), a value  
404 consistent with the proportion of proline found in the processed BcepMu (23.1%), SalMu  
405 (15.5%) and PhotoMu (13.4%) Rz1 lipoproteins (44).

406 Depending on the organism, the proteins similar to KS9 gp49 in the GenBank database  
407 have been annotated as either putative class I holins or as HNH homing endonucleases. If gp49  
408 were to act as a class I holin, it would likely function with gp22 as part of a holin/antiholin pair.  
409 These systems are used to control when the onset of lysis occurs (28). However, OCTOPUS  
410 analysis of the gp49 sequence suggests that it has no transmembrane domains, so we predict that  
411 this protein is not a holin and that some other protein encoded by KS9 may be involved in

412 controlling lysis timing. A Conserved Domain Search of the predicted gp49 sequence indicates  
413 that it belongs to the HNHc superfamily (E-value =  $8e^{-6}$ ) found in HNH homing endonucleases.  
414 Homing endonuclease genes (HEGs) are common in phage genomes. For example, T4 encodes  
415 15 homing endonucleases, 6 of which (I-TevIII and MobA-E) belong to this family (34). HEGs  
416 are referred to as selfish genetic elements. They use a mechanism called homing to copy their  
417 sequence from one place in one gene to the same place in the same gene at a different locus (10).  
418 In order to complete this process, endonucleases (such as those in the HNH family) are used to  
419 cut the DNA at a specific 15-30 bp site, which is then fixed using double-strand break repair.  
420 Further experiments are required to determine if gp49 has homing endonuclease activity or if it  
421 performs some other function during infection.

422

#### 423 Contribution of the KS9 prophage to bacterial virulence

424 In many bacterial species, prophage genes make significant contributions to the virulence  
425 of the organism. Although examples have been documented in a wide variety of Gram-negative  
426 organisms (including *V. cholerae*, *E. coli*, *Pseudomonas aeruginosa*, *Neisseria meningitidis*,  
427 *Salmonella enterica*, and *Shigella flexneri*), there is limited evidence that prophage genes  
428 contribute to virulence in *Burkholderia* species (8, 43). It has been suggested that because  
429 *Burkholderia* are not strictly pathogenic and can instead survive in a variety of both terrestrial  
430 and aquatic environments, classical toxin genes may not have provided a strong evolutionary  
431 advantage to these species (43). Instead, lysogenic conversion genes of *Burkholderia* prophages  
432 would be more likely to encode proteins that would increase the viability of the cell both in the  
433 environment and *in vivo* (43).

434 In the KS9 genome, we identified one gene, gene *32*, whose product may have an effect  
435 on the pathogenicity of LMG 21824 or a K56-2 KS9 lysogen. When the gp32 sequence was  
436 subjected to a Conserved Domain Search, the conserved domain COG3950: predicted ATP-  
437 binding protein involved in virulence was found (E-value =  $6e^{-16}$ ). To determine if the integration  
438 of KS9 as a prophage increased the pathogenicity of *B. cenocepacia* K56-2, we compared the  
439 virulence of wildtype and KS9-lysogenized K56-2 (K56-2::KS9) in the *Galleria mellonella* wax  
440 moth model. In this infection model, the 50% lethal dose (LD<sub>50</sub>) for K56-2 is 900 colony-  
441 forming units (CFU) (40). For both K56-2 and K56-2::KS9, infection with between  $10^4$  and  $10^6$   
442 CFU resulted in 100% mortality. There was no significant difference between the mortality of  
443 larvae infected with either K56-2 or K56-2::KS9 at any of the doses tested. Although gene *32*  
444 contains a domain putatively involved in virulence, these data suggest that it has no effect on the  
445 pathogenicity of KS9 lysogens.

446

#### 447 Construction and analysis of a KS9 lytic variant

448 The method used to convert KS9 into a lytic phage was to insertionally inactivate the  
449 putative KS9 phage repressor, gene *41*. It is well established that repressor mutant phages cannot  
450 stably lysogenize (45). Platt et al. (37) constructed a strain of *E. coli* expressing  $\lambda$  CI from the  
451 chromosome and lysogenized this strain with a  $\lambda$  *cI* mutant, W30 (4). When this strain was co-  
452 cultured with *E. coli* that was sensitive to  $\lambda$  infection, the numbers of sensitive *E. coli* present  
453 decreased. They proposed that this system could be used to provide continuous delivery of lytic  
454 phages *in vivo*. We wished to expand on this concept in two ways, first by showing that a lytic  
455 mutant could be constructed using genetic engineering, and second by showing that this mutant  
456 phage could be active *in vivo*.

457 Gene *41* encodes a 133 amino acid protein. According to BLASTP analysis, this protein  
458 shows 55% identity with gp52, the putative repressor protein of  $\phi$ E125 (E-value =  $4e^{-30}$ ), as well  
459 as similarity to CI-like proteins of phages BP-4795, H-19B, SfV, cdtI and a putative  
460 transcriptional repressor of phage  $\phi$ V10. A non-replicating knockout plasmid (pKL1) was  
461 constructed containing DNA flanking the KS9 gene *41* interrupted by a trimethoprim resistance  
462 cassette in a pALTER-1 ( $Tc^R$ ) backbone. Following transformation of this construct into *B.*  
463 *pyrrocinia* LMG 21824, a  $Tc^R Tp^R$  mutant (LMG 21824::pKL1, generated by a single crossover)  
464 was isolated.

465 If a double crossover event occurs that replaces the repressor gene with a  $Tp^R$  cassette,  
466 the cells should no longer be viable because the prophage will be induced in the absence of the  
467 repressor protein, resulting in lysis. We used two different assays to assess if this induction was  
468 occurring in LMG 21824::pKL1. First, we screened 1800  $Tc^R Tp^R$  LMG 21824::pKL1 colonies  
469 for loss of tetracycline resistance and maintenance of trimethoprim resistance (i.e. a double  
470 crossover without loss of viability). No  $Tc^S Tp^R$  colonies were found, suggesting that the double  
471 crossover event was lethal due to prophage induction. Second, we compared the release of K56-  
472 2-infecting phages from LMG 21824, LMG 21824::pKL1, and LMG 21824 with a mutation in  
473 KS9 gene *32* (LMG 21824 [KS9 *32*]). The number of phages released from LMG 21824::pKL1  
474 was over ten times greater than the number released from the other two strains (Figure 6),  
475 consistent with phage induction occurring in LMG 21824::pKL1 following a double crossover  
476 event. These two experiments provide further evidence that gene *41* is the repressor, as it is  
477 required to maintain stable integration of the KS9 prophage.

478 Phages isolated from culture supernatants of LMG 21824::pKL1 were screened for the  
479 presence of the  $Tp^R$  cassette. Using primers flanking gene *41*, a PCR product of 603 bp was

480 amplified with wildtype KS9, while a product of 832 bp was amplified from the mutated  
481 repressor phage with the  $Tp^R$  cassette. A representative phage isolate that tested positive during  
482 PCR screening was named KS9c. This isolate showed no defects in activity and was able to  
483 produce confluent lysis of *B. cenocepacia* K56-2 in an agar overlay at titres of  $10^7$ /ml, similar to  
484 that of wild-type KS9. The host range of KS9c was tested and it was found to be identical to that  
485 of wildtype KS9, suggesting that there was no change in the susceptibility of Bcc strains to this  
486 phage.

487 To assess if KS9c is able to stably integrate into K56-2, plates of K56-2 and KS9 or K56-  
488 2 and KS9c exhibiting confluent lysis were overlaid with water and the surviving cells were  
489 isolated. 150 bacterial isolates from KS9c lysates were replica plated onto solid medium with  
490 and without trimethoprim. These isolates were unable to grow on trimethoprim medium,  
491 suggesting that KS9c had not stably integrated into any of these bacteria. 50 KS9-insensitive and  
492 50 KS9C-insensitive K56-2 isolates were recovered from the phage lysates and were assayed for  
493 their a) growth phenotype, b) trimethoprim resistance, c) susceptibility to KS9 and KS9c and d)  
494 ability to amplify with primers designed to the K56-2/5' KS9 prophage junction. The majority of  
495 KS9-insensitive isolates (41 isolates, 82%) were non-lysogenized. These strains grew normally,  
496 were  $Tp^S$ ,  $KS9^RKS9c^R$  and were PCR negative for KS9 integration. Eighteen percent (9 isolates)  
497 were stably lysogenized. These strains grew normally, were  $Tp^S$ ,  $KS9^RKS9c^R$  and were PCR  
498 positive. A different distribution was observed for the KS9c-insensitive isolates. In this case, all  
499 50 isolates (100%) were non-lysogenized. Like the non-lysogenized KS9-insensitive isolates,  
500 these strains grew normally, were  $Tp^S$ ,  $KS9^RKS9c^R$  and were PCR negative for KS9 integration.  
501 While almost one-fifth of KS9-insensitive isolates were stably lysogenized, none of the KS9c-  
502 insensitive isolates showed this phenotype. Therefore, we have shown that inactivating prophage

503 KS9 gene *41* results in loss of lysogen viability and increased prophage induction from LMG  
504 21824 and prevention of stable lysogeny following K56-2 infection. Consequently, we conclude  
505 that gene *41* encodes the KS9 repressor protein and that KS9 is converted from a temperate to a  
506 lytic phage following loss of this gene.

507 We chose to test the efficacy of KS9c in an *in vivo* alternative infection model. Seed and  
508 Dennis (39) showed that *G. mellonella* larvae infected with twice the lethal dose of K56-2 could  
509 be rescued following administration of phage KS12 at an MOI (multiplicity of infection) of  
510 5000. We tested the efficacy of treatment with endotoxin-free KS9c lysates in K56-2-infected  
511 larvae at MOIs between 0.5 and 100. Treatment with KS9c at MOIs of 50 or 100 increased the  
512 survival of infected larvae to that of uninfected controls (Figure 7). This result is in sharp  
513 contrast to untreated infected larvae that had survival rates near zero. MOIs lower than 50 were  
514 ineffective, as larvae survival following treatment was comparable to that of untreated infected  
515 controls. In contrast to larvae treated with higher MOIs, those treated with MOIs lower than 50  
516 that remained alive 48 hours post-infection exhibited both reduced movement and signs of  
517 melanization, suggesting that the K56-2 infection had progressed but was not yet fatal. As a  
518 result, we conclude that phage treatment had little or no effect at the lower MOIs. This result is  
519 expected, as higher MOIs of lytic phages are generally more effective for therapeutic purposes  
520 (6). Our results indicate that KS9c is active in an *in vivo* model and can effectively treat  
521 experimental *B. cenocepacia* K56-2 infections when administered at an MOI of 50 or greater.

522 Because KS9c is unable to stably lysogenize K56-2 and facilitate superinfection  
523 immunity, we predicted that KS9c might be a more effective therapeutic agent than KS9. We  
524 treated K56-2-infected larvae with either KS9 or KS9c at MOIs of 50, 5 and 0.5 and compared  
525 their ability to increase larval survival. In contrast to our prediction, we found no significant

526 differences between the survival of larvae treated with the two different phages (Figure 8). In  
527 order to assess why there was no difference observed between the two treatments, we isolated  
528 K56-2 from the hemolymph of infected, KS9-treated larvae and screened these isolates for  
529 lysogeny. In contrast to the *in vitro* screening presented above where nearly 20% of insensitive  
530 isolates were stably lysogenized, 0 of 50 KS9<sup>R</sup>KS9c<sup>R</sup> K56-2 *in vivo* isolates analyzed were  
531 lysogenized based on PCR screening. Because lysogeny does not appear to make a significant  
532 contribution to KS9 resistance in the infected larvae at the MOI tested, this result explains why  
533 there was no significant difference in the *in vivo* efficacy of KS9 and KS9c. Different phage  
534 MOIs most likely caused the discrepancy observed in the proportion of lysogenized bacterial  
535 isolates obtained *in vitro* and *in vivo*. MOIs were initially higher for the *in vivo* screening (100 *in*  
536 *vivo* vs. 0.1 *in vitro*) which would tend to favor lysogeny. However, rapid infection, lysis and  
537 release of progeny phage would be predicted to increase the effective MOI *in vitro* more so than  
538 *in vivo*, leading to a greater proportion of lysogenized cells in the lysate than in the larvae (36).

539 In summary, by knocking out the putative KS9 repressor gene, we have created a  
540 functionally lytic phage named KS9c. This phage does not stably lysogenize *B. cenocepacia*  
541 K56-2 and it is effective in treating experimental infections in the *G. mellonella* model. Although  
542 it is unexpected that this phage is only as effective as the wildtype phage in this model (as  
543 opposed to more effective), we suggest that this result is due to the low level of lysogeny  
544 observed at the MOIs tested *in vivo*.

545

#### 546 Conclusion

547 We have determined the genome sequence of the siphovirus KS9, a prophage of *B.*  
548 *pyrocinia* LMG 21824. The KS9 prophage integrates into both LMG 21824 and *B. cenocepacia*

549 K56-2 in the 3' end of the GTP cyclohydrolase II gene. It is 39,896 bp in length and encodes 50  
550 genes, many of which show similarity to genes of the *Burkholderia* prophages  $\phi$ E125 and  
551  $\phi$ 1026b and an uncharacterized prophage element of *B. cenocepacia* PC184. Although one gene  
552 was identified with a putative role in pathogenicity, KS9 integration was shown to have no effect  
553 on the virulence of *B. cenocepacia* K56-2 in the *G. mellonella* model. We were able to show that  
554 *gp41* encodes the phage lysogenic repressor by developing a lytic mutant of KS9, named KS9c.  
555 Unlike KS9, KS9c was unable to stably lysogenize K56-2. Treatment of K56-2-infected *G.*  
556 *mellonella* larvae with KS9c at MOIs of 50 or greater resulted in larvae survival comparable to  
557 uninfected controls, indicating that KS9c is an effective antibacterial agent *in vivo*. As a proof-  
558 of-principle, we have shown that temperate phages can be genetically engineered to lytic form  
559 and that these engineered phages are active *in vivo*.

560 **Acknowledgements**

561           This work was funded by an operating research grant to J. J. D. from the Canadian Cystic  
 562 Fibrosis Foundation and funds from the Canadian Institutes of Health Research for the “CIHR  
 563 Team on Aerosol Phage Therapy.” K. H. L. and K. D. S. are indebted to the Natural Sciences  
 564 and Engineering Research Council of Canada for a CGS-D and PGS-D scholarship, respectively.  
 565 The authors would like to thank Dr. David DeShazer (The United States Army Medical Research  
 566 Institute for Infectious Diseases) for testing the *B. pseudomallei* and *B. mallei* host ranges and  
 567 Dr. Miguel Valvano (University of Western Ontario) for providing the *B. cenocepacia* LPS  
 568 mutants. They would also like to thank Randy Mandryk in the University of Alberta Microscopy  
 569 Service Unit and Pat Murray and Lisa Ostafichuk in the University of Alberta Molecular Biology  
 570 Service Unit.

571

572

573

574

575

576

577

578

579

580

581 **References**

- 582 1. **Ackermann, H-W.** 2005. Bacteriophage classification, p. 67-89. *In* E. Kutter and A.  
 583 Sulakvelidze (ed.), Bacteriophages: biology and applications, CRC Press, Boca Raton, FL.
- 584 2. **Ackermann, H-W.** 2001. Frequency of morphological phage descriptions in the year 2000.  
 585 *Arch. Virol.* **146**:843-857.
- 586 3. **Altschul, S. F., T. L. Madden, A. A. Schäffer, J. Zhang, Z. Zhang, W. Miller, and D. J.**  
 587 **Lipman.** 1997. Gapped BLAST and PSI-BLAST: A new generation of protein database search  
 588 programs. *Nucleic Acids Res.* **25**:3389-3402.
- 589 4. **Bassford Jr., P. J., C. Bradbeer, R. J. Kadner, and C. A. Schnaitman.** 1976. Transport of  
 590 vitamin B<sub>12</sub> in *tonB* mutants of *Escherichia coli*. *J. Bacteriol.* **128**:242-247.
- 591 5. **Berry, J., E. J. Summer, D. K. Struck, and R. Young.** 2008. The final step in the phage  
 592 infection cycle: the Rz and Rz1 lysis proteins link the inner and outer membranes. *Mol.*  
 593 *Microbiol.* **70**:341-351.
- 594 6. **Biswas, B., S. Adhya, P. Washart, B. Paul, A. N. Trostel, B. Powell, R. Carlton, and C. R.**  
 595 **Merril.** 2002. Bacteriophage therapy rescues mice bacteremic from a clinical isolate of  
 596 vancomycin-resistant *Enterococcus faecium*. *Infect. Immun.* **70**:204-210.
- 597 7. **Bottone, E. J., S. D. Douglas, A. R. Rausen, and G. T. Keusch.** 1975. Association of  
 598 *Pseudomonas cepacia* with chronic granulomatous disease. *J. Clin. Microbiol.* **1**:425-428.
- 599 8. **Boyd, E. F. and H. Brüssow.** 2002. Common themes among bacteriophage-encoded  
 600 virulence factors and diversity among the bacteriophages involved. *Trends Microbiol.* **10**:521-  
 601 529.
- 602 9. **Burkholder, W. H.** 1950. Sour skin, a bacterial rot of onion bulbs. *Phytopath.* **40**:115-117.
- 603 10. **Burt, A. and V. Koufopanou.** 2004. Homing endonuclease genes: The rise and fall and rise

- 604 again of a selfish element. *Curr. Opin. Genet. Dev.* **14**:609-615.
- 605 11. **Carver, T. J., K. M. Rutherford, M. Berriman, M-A. Rajandream, B. G. Barrell, and J.**  
606 **Parkhill.** 2005. ACT: The Artemis comparison tool. *Bioinformatics* **21**:3422-3423.
- 607 12. **Casjens, S.** 2003. Prophages and bacterial genomics: What have we learned so far? *Mol.*  
608 *Microbiol.* **49**:277-300.
- 609 13. **Coenye, T., P. Vandamme, J. J. LiPuma, J. R. W. Govan, and E. Mahenthiralingam.**  
610 2003. Updated version of the *Burkholderia cepacia* complex experimental strain panel. *J. Clin.*  
611 *Microbiol.* **41**:2797-2798.
- 612 14. **Dale, J. and S. F. Park.** 2004. *Molecular Genetics of Bacteria*, 4<sup>th</sup> edition. John Wiley and  
613 Sons, Hoboken, NJ.
- 614 15. **Dennis, J. J. and G. J. Zylstra.** 1998. Plasposons: modular self-cloning minitransposon  
615 derivatives for rapid genetic analysis of gram-negative bacterial genomes. *Appl. Environ.*  
616 *Microbiol.* **64**:2710-2715.
- 617 16 **Dennis, J. J. and G. J. Zylstra.** 1998. Improved antibiotic-resistance cassettes through  
618 restriction site elimination using *Pfu* DNA polymerase PCR. *BioTechniques* **25**:772-776.
- 619 17. **DeShazer, D.** 2004. Genomic diversity of *Burkholderia pseudomallei* clinical isolates:  
620 subtractive hybridization reveals a *Burkholderia mallei*-specific prophage in *B. pseudomallei*  
621 1026b. *J. Bacteriol.* **186**:3938-3950.
- 622 18. **Duff, A. J. A.** 2002. Psychological consequences of segregation resulting from chronic  
623 *Burkholderia cepacia* infection in adults with CF. *Thorax* **57**:756-758.
- 624 19. **Estrada-De Los Santos, P., R. Bustillos-Cristales, and J. Caballero-Mellado.** 2001.  
625 *Burkholderia*, a genus rich in plant-associated nitrogen fixers with wide environmental and  
626 geographic distribution. *Appl. Environ. Microbiol.* **67**:2790-2798.

- 627 20. **Fischetti, V. A.** 2005. The use of phage lytic enzymes to control bacterial infections, p. 321-  
 628 334. *In* E. Kutter and A. Sulakvelidze (ed.), *Bacteriophages: biology and applications*, CRC  
 629 Press, Boca Raton, FL.
- 630 21. **Folsom, B. R., P. J. Chapman, and P. H. Pritchard.** 1990. Phenol and trichloroethylene  
 631 degradation by *Pseudomonas cepacia* G4: kinetics and interactions between substrates. *Appl.*  
 632 *Environ. Microbiol.* **56**:1279-1285.
- 633 22. **Freifelder, D.M.** 1987. *Molecular Biology*, 2<sup>nd</sup> edition. Jones and Bartlett Publishers, Portola  
 634 Valley, CA.
- 635 23. **Govan, J. R. W., P. H. Brown, J. Maddison, C. J. Doherty, J. W. Nelson, M. Dodd, A. P.**  
 636 **Greening, and A. K. Webb.** 1993. Evidence for transmission of *Pseudomonas cepacia* by social  
 637 contact in cystic fibrosis. *Lancet* **342**:15-19.
- 638 24. **Hanlon, G. W.** 2007. Bacteriophages: an appraisal of their role in the treatment of bacterial  
 639 infections. *Int. J. Antimicrob. Ag.* **30**:118-128.
- 640 25. **Isles, A., I. Maclusky, and M. Corey.** 1984. *Pseudomonas cepacia* infection in cystic  
 641 fibrosis: An emerging problem. *J. Pediatr.* **104**:206-210.
- 642 26. **Juncker, A. S., H. Willenbrock, G. Von Heijne, S. Brunak, H. Nielsen, and A. Krogh.**  
 643 2003. Prediction of lipoprotein signal peptides in Gram-negative bacteria. *Protein Sci.* **12**:1652-  
 644 1662.
- 645 27. **Kropinski, A. M.** 2006. Phage therapy - Everything old is new again. *Can. J. Infect. Dis.*  
 646 *Med. Microbiol.* **17**:297-306.
- 647 28. **Kutter, E., R. Raya, and K. Carlson.** 2005. Molecular mechanisms of phage infection, p.  
 648 165-222. *In* E. Kutter and A. Sulakvelidze (ed.), *Bacteriophages: biology and applications*, CRC  
 649 Press, Boca Raton, FL.

- 650 29. **Loutet, S. A., R. S. Flannagan, C. Kooi, P. A. Sokol, and M. A. Valvano.** 2006. A  
 651 complete lipopolysaccharide inner core oligosaccharide is required for resistance of  
 652 *Burkholderia cenocepacia* to antimicrobial peptides and bacterial survival in vivo. *J. Bacteriol.*  
 653 **188**:2073-2080.
- 654 30. **Lukashin, A. V. and M. Borodovsky.** 1998. GeneMark.hmm: New solutions for gene  
 655 finding. *Nucleic Acids Res.* **26**:1107-1115.
- 656 31. **Lynch, K. H. and J. J. Dennis.** 2008. Assessment of the contribution of prophage KS9  
 657 protein gp32 to the virulence of *Burkholderia pyrrocinia* LMG 21824, abstr. W14, Banff  
 658 Conference on Infectious Diseases, Banff, AB.
- 659 32. **Mahenthiralingam, E., T. Coenye, J. W. Chung, D. P. Speert, J. R. W. Govan, P.**  
 660 **Taylor, and P. Vandamme.** 2000. Diagnostically and experimentally useful panel of strains  
 661 from the *Burkholderia cepacia* complex. *J. Clin. Microbiol.* **38**:910-913.
- 662 33. **Merril, C. R., D. Scholl, and S. L. Adhya.** 2003. The prospect for bacteriophage therapy in  
 663 Western medicine. *Nat. Rev. Drug Discov.* **2**:489-497.
- 664 34. **Miller, E. S., E. Kutter, G. Mosig, F. Arisaka, T. Kunisawa, and W. Ruger.** 2003.  
 665 Bacteriophage T4 genome. *Microbiol. Mol. Biol. Rev.* **67**:86-156.
- 666 35. **Ortega, X, A. Silipo, M. S. Saldías, C. C. Bates, A. Molinaro, and M. A. Valvano.** 2009.  
 667 Biosynthesis and structure of the *Burkholderia cenocepacia* K56-2 lipopolysaccharide core  
 668 oligosaccharide: truncation of the core oligosaccharide leads to increased binding and sensitivity  
 669 to polymyxin B. *J. Biol. Chem.* **284**:21738-21751.
- 670 36. **Payne, R. J. H. and V. A. A. Jansen.** 2001. Understanding bacteriophage therapy as a  
 671 density-dependent kinetic process. *J. Theor. Biol.* **208**:37-48.
- 672 37. **Platt, R., D. L. Reynolds, and G. J. Phillips.** 2003. Development of a novel method of lytic

- 673 phage delivery by use of a bacteriophage P22 site-specific recombination system. FEMS  
 674 Microbiol. Lett. **223**:259-265.
- 675 38. **Ren, J., M. Kotaka, M. Lockyer, H. K. Lamb, A. R. Hawkins, and D. K. Stammers.**  
 676 2005. GTP cyclohydrolase II structure and mechanism. J. Biol. Chem. **280**:36912-36919.
- 677 39. **Seed, K. D. and J. J. Dennis.** 2009. Experimental bacteriophage therapy increases survival  
 678 of *Galleria mellonella* larvae infected with clinically relevant strains of the *Burkholderia cepacia*  
 679 complex. Antimicrob. Agents Chemother. **53**:2205-2208.
- 680 40. **Seed, K. D. and J. J. Dennis.** 2008. Development of *Galleria mellonella* as an alternative  
 681 infection model for the *Burkholderia cepacia* complex. Infect. Immun. **76**:1267-1275.
- 682 41. **Seed, K. D. and J. J. Dennis.** 2005. Isolation and characterization of bacteriophages of the  
 683 *Burkholderia cepacia* complex. FEMS Microbiol. Lett. **251**:273-280.
- 684 42. **Speert, D. P., D. Henry, P. Vandamme, M. Corey, and E. Mahenthiralingam.** 2002.  
 685 Epidemiology of *Burkholderia cepacia* complex in patients with cystic fibrosis, Canada. Emerg.  
 686 Infect. Dis. **8**:181-187.
- 687 43. **Summer, E. J., J. J. Gill, C. Upton, C. F. Gonzalez, and R. Young.** 2007. Role of phages  
 688 in the pathogenesis of *Burkholderia*, or 'Where are the toxin genes in *Burkholderia* phages?'.  
 689 Curr. Opin. Microbiol. **10**:410-417.
- 690 44. **Summer, E. J., C. F. Gonzalez, T. Carlisle, L. M. Mebane, A. M. Cass, C. G. Savva, J.**  
 691 **LiPuma, and R. Young.** 2004. *Burkholderia cenocepacia* phage BcepMu and a family of Mu-  
 692 like phages encoding potential pathogenesis factors. J. Mol. Biol. **340**:49-65.
- 693 45. **Susskind, M. M. and D. Botstein.** 1978. Molecular genetics of bacteriophage P22.  
 694 Microbiol. Rev. **42**:385-413.
- 695 46. **Viklund, H. and A. Elofsson.** 2008. OCTOPUS: improving topology prediction by two-

696 track ANN-based preference scores and an extended topological grammar. *Bioinformatics*  
 697 **24**:1662-1668.

698 47. **Woods, D. E., J. A. Jeddeloh, D. L. Fritz, and D. DeShazer.** 2002. *Burkholderia*  
 699 *thailandensis* E125 harbors a temperate bacteriophage specific for *Burkholderia mallei*. *J.*  
 700 *Bacteriol.* **184**:4003-4017.

701 48. **Xu, J., R. W. Hendrix, and R. L. Duda.** 2004. Conserved translational frameshift in  
 702 dsDNA bacteriophage tail assembly genes. *Mol. Cell* **16**:11-21.

703 49. **Young, R., I-N. Wang, and W. D. Roof.** 2000. Phages will out: Strategies of host cell lysis.  
 704 *Trends Microbiol.* **8**:120-128.

705 50. **Zucker, M.** 2003. Mfold web server for nucleic acid folding and hybridization prediction.  
 706 *Nucleic Acids Res.* **31**:3406-3415.

707  
 708  
 709  
 710  
 711  
 712  
 713  
 714  
 715  
 716  
 717  
 718

719 **Figure Legends**

720

721 Figure 1 – Transmission electron micrograph of KS9. The sample was negatively stained with  
722 2% phosphotungstic acid and viewed at 180,000-fold magnification with a Philips/FEI  
723 (Morgagni) Transmission Electron Microscope.

724

725 Figure 2 – Map of the KS9 prophage. Genes transcribed in the forward direction are displayed  
726 above those transcribed in the reverse direction. Gene names are listed above and the scale (in  
727 base pairs) is shown below. The vertical extension of gene *I2* indicates the open reading frame  
728 following a translational frameshift. Gene *24'* is shown embedded in gene *24*. Abbreviation:  
729 HEG = homing endonuclease gene.

730

731 Figure 3 – Artemis Comparison Tool analysis of  $\phi$ E125,  $\phi$ 1026b, KS9 and the similar locus of  
732 *Burkholderia cenocepacia* PC184. A: comparison of  $\phi$ 1026b (above) and  $\phi$ E125 (below). B:  
733 comparison of  $\phi$ 1026b (above) and KS9 (below). C: comparison of KS9 (above) and PC184  
734 (below).

735

736 Figure 4 – Sequence of the KS9 *attP* overlap region and *attL/R* in LMG 21824. The overlapping  
737 sequence present in *attL* and *attR* of the KS9 prophage and in the chromosome of the vegetative  
738 phage (virion) is underlined.

739

740 Figure 5 – Predicted stem-loop structure downstream of the putative KS9 gp11 translational  
 741 frameshift sequence. Structure was determined using mfold analysis of the 65 bases downstream  
 742 of the AAAAAAA site (Zuker 2003).

743

744 Figure 6 – Enumeration of K56-2-infecting phages released into the supernatant from 16 hour  
 745 overnight cultures of LMG 21824, LMG 21824 (KS9 32) and LMG 21824::pKL1. Cultures were  
 746 pelleted by centrifugation at 10,000 x g for 2 minutes and the supernatant was filter sterilized  
 747 using a 0.45 µm filter and tested in a plaque assay with K56-2. This procedure was repeated  
 748 three times for each strain.

749

750 Figure 7 – Survival of K56-2-infected KS9c-treated *Galleria mellonella* 48 hours post-infection.  
 751 Larvae were infected with twice the 50% lethal dose (LD<sub>50</sub>) of K56-2 and treated with KS9c at  
 752 MOIs between 0.5 and 100. Control larvae were injected with either twice the 50% lethal dose  
 753 (LD<sub>50</sub>) of K56-2 and MgSO<sub>4</sub>/ampicillin solution or undiluted KS9c and MgSO<sub>4</sub>/ampicillin  
 754 solution. For each MOI, ten larvae were infected and treated in three separate experiments.

755

756 Figure 8 – Survival of K56-2-infected and KS9- or KS9c-treated *Galleria mellonella* 48 hours  
 757 post-infection. Larvae were infected with twice the 50% lethal dose (LD<sub>50</sub>) of K56-2 and treated  
 758 with KS9 or KS9c at an MOI of 50, 5, or 0.5. Control larvae were injected with either twice the  
 759 50% lethal dose (LD<sub>50</sub>) of K56-2 and MgSO<sub>4</sub>/ampicillin solution or undiluted KS9 or KS9c and  
 760 MgSO<sub>4</sub>/ampicillin solution. For each MOI, ten larvae were infected and treated in three separate  
 761 experiments.

762

763 Table 1 – KS9 genome annotation

gene	coding region	putative function	strand	predicted RBS and start codon	length (res.)	closest relative	alignment region (res.)	% ID	source	GenBank accession number
31	241-1515	integrase	plus	TAGTtttgcATG	424	phage integrase	1-424/424	91	<i>Bcen</i> MC0-3	YP_001779169.1
32	1658-2962	hypothetical protein	plus	ATTTGGGcatcctcatGTG	434	hypothetical protein PROVALCAL_01964	3-396/396	28	<i>Pa</i> DSM 30120	ZP_03319024.1
33	2955-3710	hypothetical protein	plus	GGAGGccttgccaATG	251	hypothetical protein CPS_0494	1-203/247	33	<i>Cp</i> 34H	YP_267252.1
34	3823-4098	transcriptional regulator	minus	GGGAgaatcaATG	91	Prophage CP4-57 regulatory protein (AlpA) family	1-76/80	59	<i>Bt</i> E264	YP_442445.1
35	4123-4947	chromosome partitioning protein	minus	AACAAAAtataaccATG	274	hypothetical protein BB1674	1-256/274	65	<i>Bb</i> RB50	NP_888219.1
36	4999-5064	hypothetical protein	minus	GAAGGAATgatcgATG	21	n/a	n/a	n/a	n/a	n/a
37	5068-5274	hypothetical protein	minus	GTGAGcaagccATG	68	hypothetical protein Bmul_4870	10-67/67	53	<i>Bm</i> ATCC 17616	YP_001584833.1

38	5282-5407	hypothetical protein	minus	ATTGAGGtgcacATG	41	n/a	n/a	n/a	n/a	n/a
39	5415-5555	hypothetical protein	minus	AGACGAGGccctgATG	46	n/a	n/a	n/a	n/a	n/a
40	5824-6111	hypothetical protein	plus	GAGGGTggggctgtgATG	95	hypothetical protein BthaB_33341	1-77/77	71	<i>Br</i> Bt4	ZP_02389868.1
41	6079-6480	repressor protein	minus	TGAAttgcagacATG	133	gp52	1- 133/133	75	<i>Br</i> Bt4	ZP_02389867.1
42	6566-6805	hypothetical protein	plus	AAAGTtgcggcATG	79	hypothetical protein BthaT_11693	1-77/80	71	<i>Br</i> TXDOH	ZP_02371673.1
43	6986-7186	hypothetical protein	minus	GGAGccgattATG	66	hypothetical protein OsJ_023465	384- 438/613	40	<i>Os</i> (japonica cultivar-group)	EAZ39982.1
44	7276-7782	hypothetical protein	plus	AAGGGtaaaaATG	168	hypothetical protein Bpse9_06757	5- 175/176	46	<i>Bp</i> 91	ZP_02446505.1
45	7810-9177	helicase	plus	GAAGAACTctgggaaacaATG	455	replicative DNA helicase	1- 455/455	60	<i>Bcen</i> PC184	YP_002091324.1
46	9223-10263	replication protein	plus	TGGCGcgcgcaATG	346	phage O protein	16- 289/319	23	<i>See</i> serovar Javiana str. GA_MM0404243 3	EDN74656

47	10274-10672	hypothetical protein	plus	GAAGAATGAcgggaaattATG	132	gp66, conserved hypothetical protein	5-133/139	41	<i>Burkholderia</i> phage $\phi$ 644-2	YP_001111145.1
48	10844-11419	hypothetical protein	plus	GGGAGAtcgttaATG	191	hypothetical protein syc0482_c	48-180/182	27	<i>Se</i> PCC 6301	YP_171192.1
49	11449-11817	homing endonuclease	plus	GGAGAgcgttaATG	122	gp82 phage protein	38-148/159	92	<i>Bcen</i> PC184	YP_002091325.1
1	12013-12516	hypothetical protein	plus	GGAAGcctcacATG	167	hypothetical protein BCPG_00011	1-167/167	91	<i>Bcen</i> PC184	YP_002091326.1
2	12561-14237	terminase	plus	GGGTATGGcctgcccGTG	558	phage terminase-like protein	62-615/615	89	<i>Bcen</i> PC184	YP_002091327.1
3	14234-15523	portal protein	plus	GGAATctacatcctATG	429	phage-related protein	1-429/429	85	<i>Bcen</i> PC184	YP_002091328.1
4	15552-16307	protease/scaffold protein	plus	GTGccttcagcGTG	251	protease subunit of ATP-dependent Clp proteases	1-251/251	93	<i>Bcen</i> PC184	YP_002091329.1
5	16376-17641	major capsid protein	plus	GATGGAGactgtATG	421	phage $\phi$ -c31 gp36-like protein	1-418/418	58	<i>Rs</i> MolK2	YP_002254489.1
6	17692-18276	hypothetical protein	plus	GTGAGGaataaATG	194	hypothetical protein RSMK01647	4-176/184	40	<i>Rs</i> MolK2	YP_002254490.1

7	18287-18613	head-tail adaptor	plus	GAGGaccgtATG	108	phage head-tail adaptor, putative	1-108/108	84	<i>Bo</i> C6786	ZP_02367135.1
8	18606-19028	hypothetical protein	plus	GAAGGTGggggagaagtATG	140	gp9	1-140/140	85	<i>Burkholderia</i> phage $\phi$ 1026b	NP_945039.1
9	19025-19369	hypothetical protein	plus	GGGGTggccgGTG	114	hypothetical protein BCPG_00017	1-114/114	86	<i>Bcen</i> PC184	YP_002091332.1
10	19429-19893	major tail subunit	plus	ATGAGGgcttATG	154	gp70	1-154/154	83	<i>Burkholderia</i> phage Bcep176	YP_355406.1
11	19922-20389	tail assembly chaperone	plus	GAAAGGAAAgagtATG	155	gp69'	8-133, 142-155/246	76, 78	<i>Bc</i> phage Bcep176	YP_355404.1
12	19922-20664	minor tail protein	plus	GAAAGGAAAgagtATG	247	gp69'	8-246/246	78	<i>Bc</i> phage Bcep176	YP_355404.1
13	20678-24778	tail length tape measure protein	plus	AGGTGGAtagaaaATG	1366	phage-related minor tail protein	1-1366/1366	97	<i>Bcen</i> PC184	YP_002091337.1
14	24778-25116	minor tail protein	plus	GGGATGgggtgATG	112	gp67	1-112/112	88	<i>Burkholderia</i> phage Bcep176	YP_355402.1
15	25126-26934	hypothetical protein	plus	ATAGGGtagaaaATG	602	gp66	1-193/335	52	<i>Bc</i> phage Bcep176	YP_355401.1

16	26939-27622	minor tail protein	plus	GAGTTAgccatATG	227	gp65 phage protein	1-227/227	92	<i>Bcen</i> PC184	YP_002091339.1
17	27672-28424	tail component protein	plus	GGGTTtttttATG	250	hypothetical protein BCPG_00025	1-250/250	95	<i>Bcen</i> PC184	YP_002091340.1
18	28421-28984	tail component protein	plus	GGGGTgcgaaGTG	187	gp63 phage protein	1-187/187	97	<i>Bcen</i> PC184	YP_002091341.1
19	28981-32889	tail tip fiber protein	plus	AGAGGAtcaagtGTG	1302	phage-related protein, tail component	1-1300/1301	92	<i>Bcen</i> PC184	YP_002091342.1
20	32886-33194	hypothetical protein	plus	GGGGGAGGtgggcGTG	102	hypothetical protein BTH_III1063	3-104/104	95	<i>Br</i> E264	YP_439260.1
21	33194-33910	hypothetical protein	plus	GGAGTGtattaATG	238	hypothetical protein BTH_III1064	9-246/246	93	<i>Br</i> E264	YP_439261.1
22	33910-34248	holin	plus	GGGAATTgtgtgATG	112	holin	36-147/147	94	<i>Br</i> E264	YP_439262.1
23	34251-34700	endolysin	plus	GGAGAAAAataaacATG	149	hypothetical protein BTH_III1066	1-149/149	92	<i>Br</i> E264	YP_439263.1
24	34697-35179	Rz	plus	CGGAGgggctATG	160	gp23 phage protein	1-160/160	81	<i>Bcen</i> PC184	YP_002091345.1

24'	34896-35159	Rz1	plus	AGGGGGAacgctgaagATG	87	hypothetical protein Bamb_1851	6-92/180	65	<i>Bc</i> AMMD	YP_773741.1
25	35318-36109	DNA adenine methylase	plus	AAATACGGettcacaATG	263	DNA adenine methylase	1- 262/262	87	<i>Bp</i> 1106b	ZP_02107289.1
26	36211-37107	hypothetical protein	plus	TGAGAacacaATG	298	hypothetical protein BTH_III1069	1- 298/298	93	<i>Bt</i> E264	YP_439266.1
27	37131-37622	hypothetical protein	minus	GGGAtaacactGTG	163	hypothetical protein BCPG_00032	1- 162/163	75	<i>Bcen</i> PC184	YP_002091347.1
28	37677-38312	hypothetical protein	plus	AGGGGAGeggtctATG	211	hypothetical protein BthaT_29201	1- 210/214	89	<i>Bt</i> TXDOH	ZP_02375127.1
29	38440-39201	hypothetical protein	minus	AGAGGCTcattcccATG	253	hypothetical protein SCP1.182	118- 238/251	49	<i>Sc</i> A3(2)	NP_639763.1
30	39194-39565	hypothetical protein	minus	TGCGGAAcgaacATG	123	ribonuclease G/E	296- 393/611	28	<i>Pmm</i> str. CCMP1375	NP_876048.1

764 Abbreviations: RBS = ribosome binding site; res. = amino acid residues; ID = identity; n/a = not applicable; *Ba* = *Bordetella avium*;

765 *Bb* = *Bordetella bronchiseptica*; *Bc* = *Burkholderia cepacia*; *Bcen* = *Burkholderia cenocepacia*; *Bm* = *Burkholderia multivorans*; *Bo* =

766 *Burkholderia oklahomensis*; *Bp* = *Burkholderia pseudomallei*; *Bt* = *Burkholderia thailandensis*; *Cp* = *Colwellia psychrerythraea*; *Os* =

767 *Oryza sativa*; *Pmm* = *Prochlorococcus marinus* subsp. *marinus*; *Pa* = *Providencia alcalifaciens*; *Rs* = *Ralstonia solanacearum*; *See* =

768 *Salmonella enterica* subsp. *enterica*; *Sc* = *Streptomyces coelicolor*; *Se* = *Synechococcus elongatus*. Putative functions were assigned  
769 based on BLASTX results.

770

771

772

773

774

775

776

777

778

779

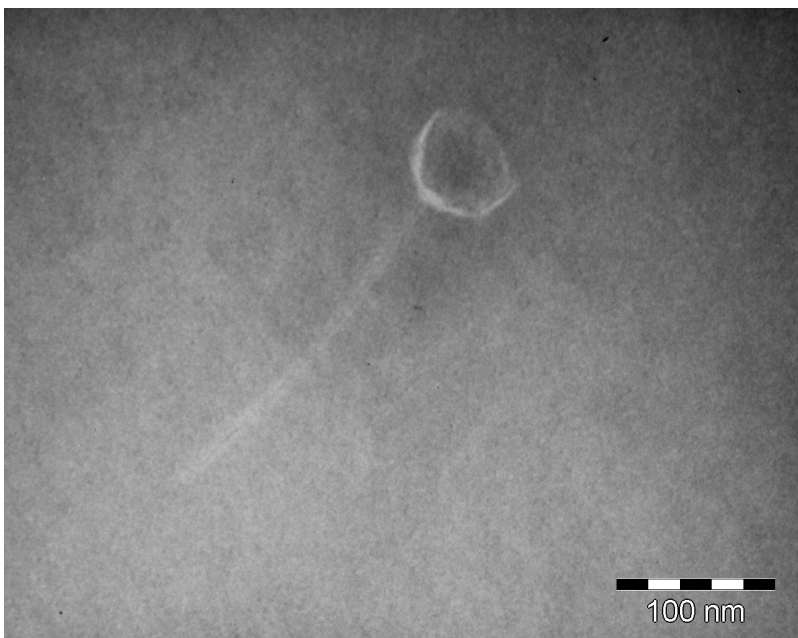
780

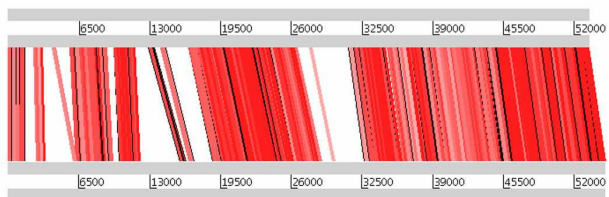
781

782

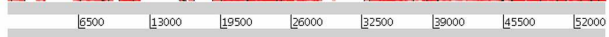
783

784

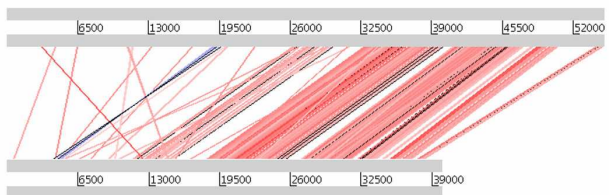




phiE125



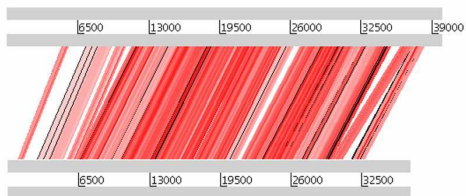
phi1026b



phi1026b



KS9



KS9



PC184

*attL* TCGGGCATTCTTCGAGGAAAACGAGTAACGTAATCAAGG  
*virion* AATGTTGTTTCTTCGAGGAAAACGAGTAACGTAATCAAGG  
*attR* AATGTTGTTTCTTCGAGGAAAACGAGTAACCGCCACGAGC



